First Exclusive Measurement of Deeply Virtual Compton Scattering off ^{4}He: Toward the 3D Tomography of Nuclei

M. Hattawy,[1,22] N.A. Baltzell,[1,37] R. Dupré,[1,22,*] K. Hafidi,[1] S. Stepanyan,[37] S. Bültmann,[31] R. De Vita,[19] A. El Alaoui,[1,38] L. El Fassi,[27] H. Egiyan,[37] F.X. Girod,[37] M. Guidal,[22] D. Jenkins,[43] S. Liuti,[42] Y. Perrin,[26] B. Torayev,[31] E. Voutier,[26,22] K.P. Adhikari,[27] S. Adhikari,[12] D. Adikaram,[31,†] Z. Akbar,[13] M.J. Amaryan,[31] S. Anefalos Pereira,[18] Whitney R. Armstrong,[1] H. Avakian,[37] J. Ball,[7] M. Bashkanov,[39] M. Battaglieri,[19] V. Batourine,[37] I. Bedlinskiy,[23] A.S. Biselli,[10] S. Boiarinov,[37] W.J. Briscoe,[15] W.K. Brooks,[38] V.D. Burkert,[37] Frank Thanh Cao,[9] D.S. Carman,[37] A. Celentano,[19] G. Charles,[31] T. Chetry,[30] G. Ciullo,[17,11] L. Clark,[40] L. Colaneri,[22] P.L. Cole,[16] M. Contalbrigo,[17] O. Cortes,[16] V. Crede,[13] A. D'Angelo,[20,33] N. Dashyan,[45] E. De Sanctis,[18] A. Deur,[37] C. Djalali,[35] L. Elouadrhiri,[37] P. Eugenio,[13] G. Fedotov,[35,34] S. Fegan,[40,‡] R. Fersch,[8,44] A. Filippi,[21] J.A. Fleming,[39] T.A. Forest,[16] A. Fradi,[22,§] M. Garçon,[7] N. Gevorgyan,[45] Y. Ghandilyan,[45] G.P. Gilfoyle,[32] K.L. Giovanetti,[24] C. Gleason,[35] W. Gohn,[9,¶] E. Golovatch,[34] R.W. Gothe,[35] K.A. Griffioen,[44] L. Guo,[12,37] H. Hakobyan,[38,45] C. Hanretty,[37,13] N. Harrison,[37] D. Heddle,[8,37] K. Hicks,[30] M. Holtrop,[28] S.M. Hughes,[39] D.G. Ireland,[40] B.S. Ishkhanov,[34] E.L. Isupov,[34] H. Jiang,[35] K. Joo,[9] S. Joosten,[36] D. Keller,[42,30] G. Khachatryan,[45] M. Khachatryan,[31] M. Khandaker,[29,**] A. Kim,[9] W. Kim,[25] A. Klein,[31] F.J. Klein,[6] V. Kubarovsky,[37] S.E. Kuhn,[31] S.V. Kuleshov,[38,23] L. Lanza,[20] P. Lenisa,[17] K. Livingston,[40] H.Y. Lu,[35] I .J .D. MacGregor,[40] N. Markov,[9] M. Mayer,[31] M.E. McCracken,[5] B. McKinnon,[40] C.A. Meyer,[5] Z.E. Meziani,[36] T. Mineeva,[38,9] M. Mirazita,[18] V. Mokeev,[37] R.A. Montgomery,[40] H. Moutarde,[7] A Movsisyan,[17] C. Munoz Camacho,[22] P. Nadel-Turonski,[37] L.A. Net,[35] S. Niccolai,[22] G. Niculescu,[24] I. Niculescu,[24] M. Osipenko,[19] A.I. Ostrovidov,[13] M. Paolone,[36] R. Paremuzyan,[28,45] K. Park,[37,35] E. Pasyuk,[37,2] E. Phelps,[35] W. Phelps,[12] S. Pisano,[18,22] O. Pogorelko,[23] J.W. Price,[3] Y. Prok,[31,42] D. Protopopescu,[40] M. Ripani,[19] B.G. Ritchie,[2] A. Rizzo,[20,33] G. Rosner,[40] P. Rossi,[37,18] F. Sabatié,[7] C. Salgado,[29] R.A. Schumacher,[5] E. Seder,[9] Y.G. Sharabian,[37] A. Simonyan,[45] Iu. Skorodumina,[35,34] G.D. Smith,[39] D. Sokhan,[40,39] N. Sparveris,[36] S. Strauch,[35] M. Taiuti,[14,‡] M. Ungaro,[37,9] H. Voskanyan,[45] N.K. Walford,[6] D.P. Watts,[39] X. Wei,[37] L.B. Weinstein,[31] M.H. Wood,[4] N. Zachariou,[39] L. Zana,[39,28] J. Zhang,[42] and Z.W. Zhao[31,35]

(The CLAS Collaboration)

[1] *Argonne National Laboratory, Argonne, Illinois 60439*
[2] *Arizona State University, Tempe, Arizona 85287-1504*
[3] *California State University, Dominguez Hills, Carson, CA 90747*
[4] *Canisius College, Buffalo, NY*
[5] *Carnegie Mellon University, Pittsburgh, Pennsylvania 15213*
[6] *Catholic University of America, Washington, D.C. 20064*
[7] *Irfu/SPhN, CEA, Université Paris-Saclay, 91191 Gif-sur-Yvette, France*
[8] *Christopher Newport University, Newport News, Virginia 23606*
[9] *University of Connecticut, Storrs, Connecticut 06269*
[10] *Fairfield University, Fairfield CT 06824*
[11] *Universita' di Ferrara , 44121 Ferrara, Italy*
[12] *Florida International University, Miami, Florida 33199*
[13] *Florida State University, Tallahassee, Florida 32306*
[14] *Università di Genova, 16146 Genova, Italy*
[15] *The George Washington University, Washington, DC 20052*
[16] *Idaho State University, Pocatello, Idaho 83209*
[17] *INFN, Sezione di Ferrara, 44100 Ferrara, Italy*
[18] *INFN, Laboratori Nazionali di Frascati, 00044 Frascati, Italy*
[19] *INFN, Sezione di Genova, 16146 Genova, Italy*
[20] *INFN, Sezione di Roma Tor Vergata, 00133 Rome, Italy*
[21] *INFN, Sezione di Torino, 10125 Torino, Italy*
[22] *Institut de Physique Nucléaire, CNRS/IN2P3 and Université Paris Sud, 91406 Orsay, France*
[23] *Institute of Theoretical and Experimental Physics, Moscow, 117259, Russia*
[24] *James Madison University, Harrisonburg, Virginia 22807*
[25] *Kyungpook National University, Daegu 41566, Republic of Korea*
[26] *LPSC, Université Grenoble-Alpes, CNRS/IN2P3, 38026 Grenoble, France*
[27] *Mississippi State University, Mississippi State, MS 39762-5167*
[28] *University of New Hampshire, Durham, New Hampshire 03824-3568*
[29] *Norfolk State University, Norfolk, Virginia 23504*
[30] *Ohio University, Athens, Ohio 45701*

[31] Old Dominion University, Norfolk, Virginia 23529
[32] University of Richmond, Richmond, Virginia 23173
[33] Universita' di Roma Tor Vergata, 00133 Rome Italy
[34] Skobeltsyn Institute of Nuclear Physics, Lomonosov Moscow State University, 119234 Moscow, Russia
[35] University of South Carolina, Columbia, South Carolina 29208
[36] Temple University, Philadelphia, PA 19122
[37] Thomas Jefferson National Accelerator Facility, Newport News, Virginia 23606
[38] Universidad Técnica Federico Santa María, Casilla 110-V Valparaíso, Chile
[39] Edinburgh University, Edinburgh EH9 3JZ, United Kingdom
[40] University of Glasgow, Glasgow G12 8QQ, United Kingdom
[41] Virginia Tech, Blacksburg, Virginia 24061-0435
[42] University of Virginia, Charlottesville, Virginia 22901
[43] Virginia Polytechnic Institute and State University, Blacksburg, Virginia, 24061
[44] College of William and Mary, Williamsburg, Virginia 23187-8795
[45] Yerevan Physics Institute, 375036 Yerevan, Armenia

We report on the first measurement of the beam-spin asymmetry in the exclusive process of coherent deeply virtual Compton scattering off a nucleus. The experiment uses the 6 GeV electron beam from the Continuous Electron Beam Accelerator Facility (CEBAF) accelerator at Jefferson Lab incident on a pressurized ^{4}He gaseous target placed in front of the CEBAF Large Acceptance Spectrometer (CLAS). The scattered electron is detected by CLAS and the photon by a dedicated electromagnetic calorimeter at forward angles. To ensure the exclusivity of the process, a specially designed radial time projection chamber is used to detect the recoiling ^{4}He nuclei. We measure beam-spin asymmetries larger than those observed on the free proton in the same kinematic domain. From these, we are able to extract, in a model-independent way, the real and imaginary parts of the only ^{4}He Compton form factor, $\mathcal{H}_A$. This first measurement of coherent deeply virtual Compton scattering on the ^{4}He nucleus, with a fully exclusive final state via nuclear recoil tagging, leads the way toward 3D imaging of the partonic structure of nuclei.

The generalized parton distribution (GPD) framework offers the opportunity to obtain information about the momentum and spatial degrees of freedom of the quarks and gluons inside hadrons [1–5]. In impact parameter space the GPDs are indeed interpreted as a tomography of the transverse plane for partons carrying a given fraction of the proton longitudinal momentum [6–9]. The most promising way to access GPDs experimentally is through the measurement of deeply virtual Compton scattering (DVCS), i.e., the hard exclusive electroproduction of a real photon on a hadron. While other processes are also known to be sensitive to GPDs, the measurement of DVCS is considered the cleanest probe and has been the focus of efforts at Jefferson Lab, HERA, and CERN [10–25]. The vast majority of these measurements focused on the study of the proton and allowed for an extraction of its three-dimensional image (for reviews of the field, see [26–31]). These recent developments could also be applicable to nuclei, giving access to novel information about nuclear structure in terms of quarks and gluons [32–35]. Such a study of the 3D structure of nuclei appears to be especially interesting in light of the large, yet unresolved, nuclear effects observed in nuclear parton distribution functions [36–38]. The results presented in this Letter demonstrate the feasibility of such an approach and constitute the first step toward a tomography of nuclei.

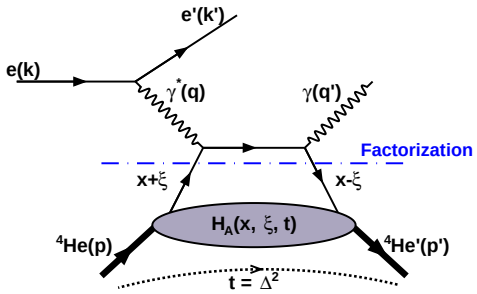

FIG. 1: Representation of the leading-order handbag diagram of the DVCS process off ^{4}He.

Figure 1 illustrates the handbag diagram for coherent DVCS on ^{4}He, where the four-vectors of the electrons, photons, and ^{4}He are denoted by k/k', q/q', and p/p', respectively. For large virtual photon 4-momentum squared, $Q^2 = -(k-k')^2$, and small squared momentum transfer, $t = (p-p')^2$, the DVCS handbag diagram can be factorized into two parts [39, 40]. The hard part includes the photon-quark interaction and is calculable in pertur-

*corresponding author: dupre@ipno.in2p3.fr
†Current address:Thomas Jefferson National Accelerator Facility, Newport News, Virginia 23606
‡Current address:INFN, Sezione di Genova, 16146 Genova, Italy
§Current address:Faculty of Sciences of Gabes, Department of Physics, 6072-Gabes, Tunisia
¶Current address:University of Kentucky, Lexington, Kentucky 40506
**Current address:Idaho State University, Pocatello, Idaho 83209

bative QED. The nonperturbative part is parametrized in terms of GPDs, which embed the partonic structure of the hadron. The GPDs depend on the three variables x, ξ, and t. ξ relates to the Bjorken variable x_A: $\xi \approx \frac{x_A}{2-x_A}$, where $x_A = \frac{Q^2}{2M_A\nu}$, ν is the energy of the virtual photon, and M_A is the nuclei mass. x is the quark's internal loop momentum fraction and cannot be accessed experimentally in DVCS. We in fact measure Compton form factors (CFFs), which are complex quantities defined as

$$\Re(\mathcal{H}_A) = \mathcal{P}\int_0^1 dx[H_A(x,\xi,t) - H_A(-x,\xi,t)]\,C^+(x,\xi), \quad (1)$$

$$\Im(\mathcal{H}_A) = -\pi[H_A(\xi,\xi,t) - H_A(-\xi,\xi,t)], \quad (2)$$

with H_A a GPD, $\mathcal{P}$ the Cauchy principal value integral, and a coefficient function $C^+ = 1/(x-\xi) + 1/(x+\xi)$.

Until now, the only available data on nuclear DVCS were from the HERMES experiment [12]. In this experiment, the exclusivity of the reaction was obtained through kinematic cuts using only the measured scattered electron and real photon. This measurement was performed on a large set of nuclei (^{4}He, ^{14}N, ^{20}Ne, ^{85}Kr, and ^{131}Xe), but contamination from incoherent processes can be suspected to influence the results significantly [41]. The direct detection of the recoil nucleus can, however, guarantee that the nucleus remains intact.

The ^{4}He nucleus is an ideal experimental target for nuclear DVCS, as it is light enough to be detected by our experimental setting, while it is subject to interesting nuclear effects [42]. Its zero spin also leads to an important simplification, as a spin-zero hadron is parametrized by only one chiral even GPD $[H_A(x,\xi,t)]$ at leading twist, while four GPDs arise for the spin-$\frac{1}{2}$ nucleon. This significantly simplifies the interpretation of the data and allows a model-independent extraction of the ^{4}He CFF ($\mathcal{H}_A$) presented at the end of this Letter.

The Continuous Electron Beam Accelerator Facility (CEBAF) Large Acceptance Spectrometer (CLAS) in Hall B at Jefferson Lab [43] has been previously supplemented with an inner calorimeter (IC) and a solenoid magnet to measure DVCS observables on the nucleon [18, 20, 21, 23, 24]. The IC extended the photon detection acceptance of CLAS to polar angles as low as 4°. The 5-T solenoid magnet acted as a guiding field for the low-energy Møller electrons that were absorbed in a heavy shield placed around the beam line.

In the kinematic range of the present experiment, the recoil ^{4}He nuclei have low momentum, averaging 300 MeV. CLAS could not detect such low-energy α particles, so, in order to ensure the exclusivity of the measurement, we built a small and light radial time projection chamber (RTPC). The RTPC was a 20-cm-long cylinder with a diameter of 15 cm, positioned in the solenoid magnet. In the center of the RTPC was the target cell, a 25-cm-long and 6-mm-diameter Kapton tube with 27-μm-thick walls filled with gaseous ^{4}He at 6 atm (see [44] for a detailed description of the RTPC and its performances). The experiment (E08-024) [45] collected data over 40 days at the end of 2009 using a nearly 100% duty factor, longitudinally polarized electron beam (83.7±3.5% polarization [46]) at an energy of 6.064 GeV. The RTPC was calibrated specifically for the detection of ^{4}He nuclei using elastic scattering ($e^4\mathrm{He} \rightarrow e'^4\mathrm{He}'$) with a 1.2 GeV electron beam.

To identify coherent DVCS events, we first selected events where one electron, one ^{4}He, and at least one photon were detected in the final state. Electrons were identified using their measured momentum, light yield, time, and energy obtained from the CLAS drift chambers, Čerenkov counters, scintillator counters, and electromagnetic calorimeters, respectively. The recoiling ^{4}He nuclei were identified in the RTPC using time and energy-loss cuts for tracks in the fiducial region [47]. In addition, we applied a vertex-matching cut to ensure that the electron and helium nucleus originated from a common reaction vertex in the target cell. The photons were detected in either the IC or the CLAS electromagnetic calorimeters. Note that even though the DVCS reaction has only one real photon in the final state, events with more than one good photon were not discarded at this stage. These were mainly caused by accidental coincidences of soft photons and did not directly affect this measurement, as only the most energetic photon of an event was considered a DVCS photon candidate. This prescription, however, slightly increased the corrections associated with the π^0 and the accidental backgrounds discussed below.

We selected events with Q^2 greater than 1 GeV^2 for which the DVCS handbag diagram is believed to be dominant. Then the exclusivity of the reaction was ensured by applying a set of cuts on the following kinematic variables: the coplanarity angle $\Delta\phi$ between the (γ,γ^*) and $(\gamma^*,{}^4\mathrm{He}')$ planes, the missing energy, mass, and transverse momentum of the $e'^4\mathrm{He}'\gamma$ system, the missing mass squared of the $e'^4\mathrm{He}'$ system, and the angle θ between the measured photon and the missing momentum of the $e'^4\mathrm{He}'$ system. The experimental data for the most relevant exclusivity variables and applied cuts are shown in Fig. 2 (see [47] for additional details). We also rejected events where a π^0 was identified by the invariant mass of two photons. About 3200 events passed all these requirements; their kinematic distributions are shown in Fig. 3. (We use here and for other results $x_B = \frac{Q^2}{2M_N\nu}$ with M_N the proton mass instead of x_A. This makes it easier to compare these results with the proton DVCS data available in the literature.)

We identified two main backgrounds: accidental coincidences and exclusive coherent π^0 production. The accidentals have particles originating from different events, and we estimated their contribution to be 4.1% of the

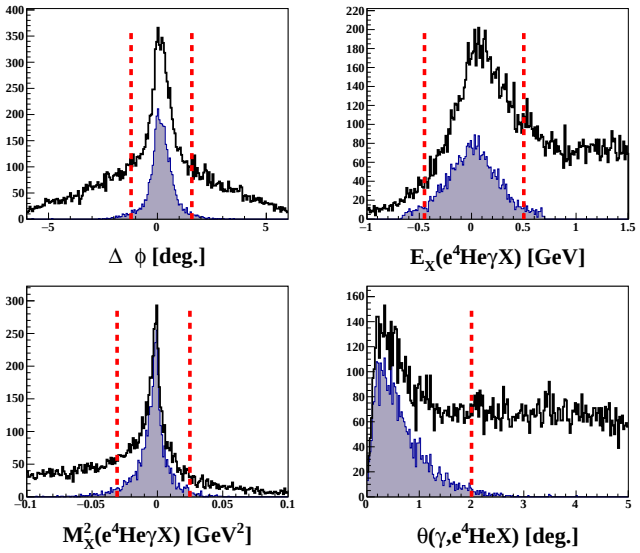

FIG. 2: Four of the six coherent DVCS exclusivity cuts. The black distributions represent the initial candidate events, while the shaded distributions represent those that passed all of the exclusivity cuts except the quantity plotted. The vertical red lines represent the applied cuts. The distributions from left to right and from top to bottom are coplanarity angle $\Delta\phi$, missing energy E_X, missing mass squared M_X^2, and the cone angle θ between the measured photon and the missing momentum of the $e'^4\mathrm{He}'$ system.

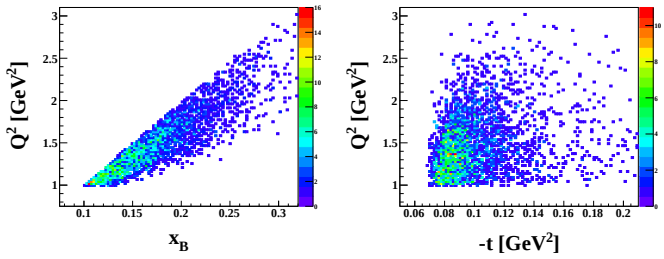

FIG. 3: Coherent DVCS event distributions for Q^2 after exclusivity cuts. The distributions are shown as a function of Bjorken variable x_B (left) and as a function of squared-momentum transfer $-t$ (right).

data sample. We evaluated this contribution by selecting events passing all the cuts but with the scattered electron and ^{4}He originating from different vertices. The π^0 production can be mistaken for DVCS when one of the two photons from the π^0 decay is produced at low energy in the laboratory frame and remains undetected. To estimate the effect of this contamination, we developed an event generator tuned on the experimental yield of exclusive π^0 with two photons measured. We used this generator together with a GEANT3 simulation of our detectors to estimate the ratio of the number of π^0 events where the two photons are detected to those that are misidentified as DVCS events. This ratio is then multiplied by the measured yield of exclusive π^0 events to correct the DVCS data. Depending on the kinematics, we found contaminations of 2-4%.

In this work, the physics observable extracted using coherent DVCS events is the beam-spin asymmetry A_{LU}. On an unpolarized target, A_{LU} is defined as the difference of cross sections for the reaction with opposite beam helicities normalized to the total cross section:

$$A_{LU} = \frac{d^4\sigma^+ - d^4\sigma^-}{d^4\sigma^+ + d^4\sigma^-}, \tag{3}$$

where $d^4\sigma^\pm$ is the DVCS differential cross section for positive (negative) beam helicity.

In this ratio, luminosity normalization and detector efficiencies largely cancel, and A_{LU} can be extracted from the reaction yields for the two helicities ($N^\pm$):

$$A_{LU} = \frac{1}{P_B}\frac{N^+ - N^-}{N^+ + N^-}, \tag{4}$$

where P_B is the degree of longitudinal polarization of the incident electron beam.

There is an additional process contributing to the same final state as the DVCS, the so-called Bethe-Heitler (BH) process, where the real photon is emitted by the incoming or the outgoing lepton. The DVCS and BH processes are indistinguishable experimentally, and the amplitude of the electroproduction of a real photon includes a sum of the amplitudes of these two processes. The BH amplitude depends on the target elastic form factors, which are well known in this kinematic region, while the DVCS amplitude depends on the GPDs. In our kinematics, the cross section of the real photon electroproduction is dominated by the BH contribution, which varies strongly with ϕ, the azimuthal angle between the (e, e') and $(\gamma^*, ^4\mathrm{He}')$ planes. The DVCS contribution is smaller by about a factor of 2 but independent of ϕ at twist-2 contributions with a cross section measurement. However, the DVCS-BH interference term offers an easier experimental access by generating spin asymmetries. We have, in particular, for a spin-zero target the beam spin asymmetry A_{LU}, which can be expressed at leading order and leading twist [49, 50] as

$$A_{LU}(\phi) = \frac{\alpha_0(\phi)\,\Im(\mathcal{H}_A)}{\alpha_1(\phi) + \alpha_2(\phi)\,\Re(\mathcal{H}_A) + \alpha_3(\phi)\left[\Re(\mathcal{H}_A)^2 + \Im(\mathcal{H}_A)^2\right]}. \tag{5}$$

Explicit expressions of the kinematic factors α_i are de-

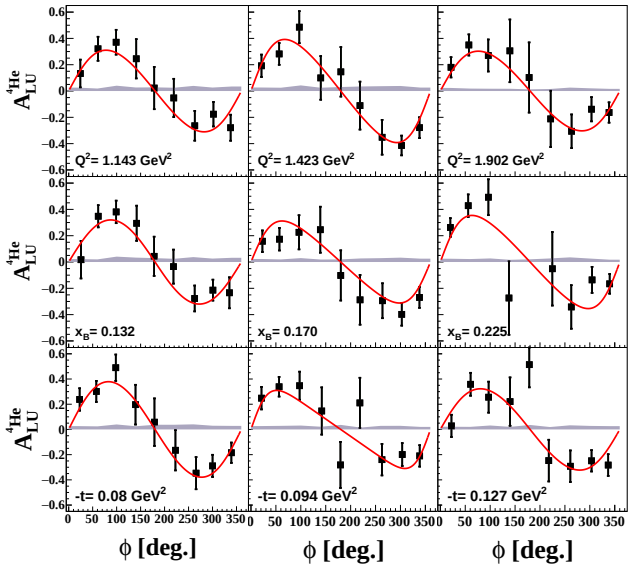

FIG. 4: A_{LU} as a function of azimuthal angle ϕ. Results are presented for different Q^2 bins (top panel), x_B bins (middle panel), and t bins (bottom panel). The error bars represent the statistical uncertainties. The gray bands represent the systematic uncertainties, including the normalization uncertainties. The red curves are the results of fits with Eq. (5).

rived from expressions in Ref. [50]:

$$\begin{aligned}
\alpha_0(\phi) &= \frac{x_A(1+\epsilon^2)^2}{y} S_{++}(1)\sin(\phi),\\
\alpha_1(\phi) &= c_0^{BH} + c_1^{BH}\cos(\phi) + c_2^{BH}\cos(2\phi),\\
\alpha_2(\phi) &= \frac{x_A(1+\epsilon^2)^2}{y}\left[C_{++}(0) + C_{++}(1)\cos(\phi)\right],\\
\alpha_3(\phi) &= \frac{x_A^2 t(1+\epsilon^2)^2}{y}\mathcal{P}_1(\phi)\mathcal{P}_2(\phi)\cdot 2\frac{2-2y+y^2+\frac{\epsilon^2}{2}y^2}{1+\epsilon^2},
\end{aligned} \tag{6}$$

where $S_{++}(1)$ and $C_{++}(0,1)$ are the Fourier harmonics of the interference amplitude in the leptonic tensor, $c_{0,1,2}^{BH}$ the Fourier harmonics of the BH amplitude, and finally $\mathcal{P}_{1,2}(\phi)$ the BH propagators, which include $\cos(\phi)$ dependencies. (The explicit expression of all these terms can be found in Appendix A of Ref. [51].). We observe that, using the different $\sin(\phi)$, $\cos(\phi)$, and $\cos(2\phi)$ contributions, one can extract unambiguously both the imaginary and real parts of $\mathcal{H}_A$ with a fit of the $A_{LU}(\phi)$ distribution.

We present in Fig. 4 A_{LU} as a function of azimuthal angle ϕ and the kinematical variables Q^2, x_B, and t. Because of limited statistics, these latter variables are studied separately with a two-dimensional data binning. The curves on the plots are fits using the function presented in Eq. (5), where the real and imaginary parts of the CFF $\mathcal{H}_A$ are the only free parameters.

Studies of systematic uncertainties showed that the main contributions come from the choice of DVCS exclusivity cuts (8% systematic uncertainty) and the large binning size (5.1%). These values are relative and quoted for A_{LU} at $\phi = 90°$. Added quadratically, the total systematic uncertainty is about 10% at 90° (or 0.03, absolute), which is significantly smaller than the statistical uncertainties at all kinematical bins.

In Fig. 5, the Q^2, x_B, and t dependencies of the fitted A_{LU} at $\phi = 90°$ are shown. The comparison to HERMES data shows that we obtain the same sign, but the size of the error bars and the difference of kinematics do not permit us to say much more. The x_B and t dependencies are also compared to theoretical calculations by Liuti and Taneja [52]. The model accounts for the effect of the nucleon virtuality (off-shellness) on the quark distribution. The calculations are at slightly different kinematics than the data but still allow us to draw some conclusions. The model appears to predict smaller asymmetries than observed. The difference may arise from the theoretical uncertainty in the determination of the crossing point where the parton nuclear distribution becomes larger than the nucleon one and reverses the sign of the nuclear effect.

The Q^2, x_B, and t dependencies of the ^{4}He CFF $\mathcal{H}_A$ extracted from the fit to the azimuthal dependence of A_{LU} are shown in Fig. 6. The curves on the graphs are model calculations, labeled *convolution* and *off-shell*. In the convolution model [53], the nucleus is assumed to be composed of nonrelativistic nucleons, each interacting independently with the probe. The convolution-dual model is based on nucleon GPDs from the dual parametrization [54], where the convolution-VGG uses nucleon GPDs from the VGG model [55] and is based on the double distributions ansatz [56]. The off-shell model is the same as in Fig. 5 using a more recent GPD model for the nucleon [57].

The results in Fig. 6 show that the extraction of the CFF from the A_{LU} is possible without model-dependent assumptions beyond leading-twist and leading-order dominance. The amplitude and the dependencies observed as a function of Q^2, x_B, and t are in agreement with the theoretical expectations. One can see a difference between the precision of the extracted imaginary and real parts, which is due to α_2 being much smaller than α_1 in Eq. (5). While the precision of this measurement is not at a sufficient level to discriminate between the models, these results demonstrate the possibility of extracting the CFF of a spin-0 target directly from a A_{LU} measurement.

In summary, we have presented the first measurement of the beam-spin asymmetry of exclusive coherent DVCS off ^{4}He using the CLAS spectrometer supplemented with a RTPC. This setup allowed detection of the low-energy ^{4}He recoils in order to ensure an exclusive measurement of the coherent DVCS process. The azimuthal dependence of the measured A_{LU} has been used to extract, in a model-independent way, the real and the imaginary

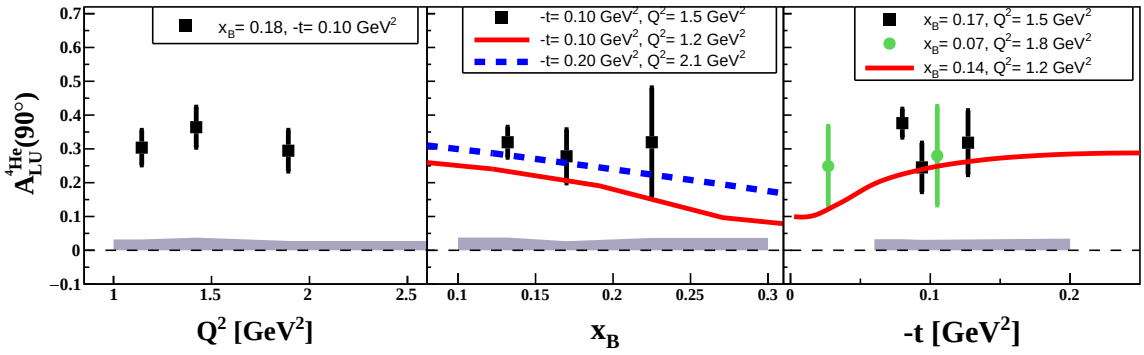

FIG. 5: The Q^2 (left), x_B (middle), and t dependencies (right) of A_{LU} at $\phi = 90°$ (black squares). In the middle plot, the full red and the dashed blue curves are theoretical calculations from Ref. [52]. On the right, the green circles are the HERMES $-A_{LU}$ (a positron beam was used) inclusive measurements [12], and the curve is the theoretical calculation from Ref. [52]. The gray bands represent the systematic errors.

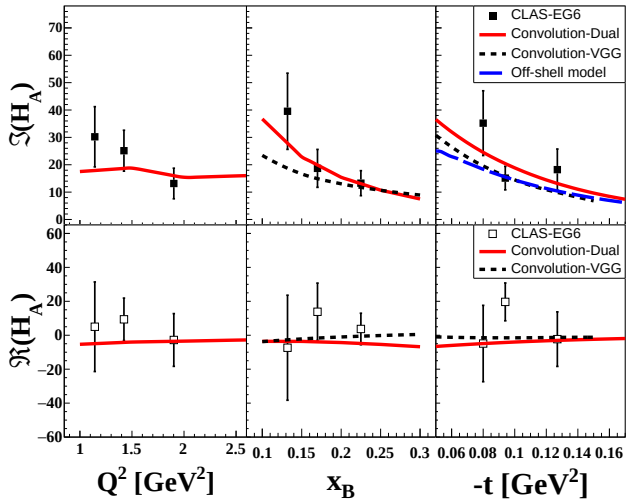

FIG. 6: The leading-twist model-independent extraction of the imaginary (top panel) and real (bottom panel) parts of the ^{4}He CFF $\mathcal{H}_A$, as a function of Q^2 (left panel), x_B (middle panel), and t (right panel). The full red curves are the calculations based on the convolution model from Ref. [53]. The black dashed curves are calculations from the same model using different GPDs for the nucleons [Vanderhaeghen-Guichon-Guidal (VGG) model [55]]. The blue long-dashed curve on the top-right plot is from the off-shell model as described in Ref. [57].

parts of the ^{4}He CFF, $\mathcal{H}_A$. The extracted CFF is in agreement with predictions of the available models. This first fully exclusive experiment opens new perspectives for studying nuclear structure with the GPD framework and paves the way for future measurements at JLab using 12 GeV CEBAF and upgraded equipment [51].

The authors thank the staff of the Accelerator and Physics Divisions at the Thomas Jefferson National Accelerator Facility who made this experiment possible. This work was supported in part by the Chilean Comisión Nacional de Investigación Científica y Tecnológica (CONICYT), the Italian Instituto Nazionale di Fisica Nucleare, the French Centre National de la Recherche Scientifique, the French Commissariat à l'Energie Atomique, the U.S. Department of Energy under Contract No. DE-AC02-06CH11357, the United Kingdom Science and Technology Facilities Council (STFC), the Scottish Universities Physics Alliance (SUPA), the National Research Foundation of Korea, and the Office of Research and Economic Development at Mississippi State University. M. Hattawy also acknowledges the support of the Consulat Général de France à Jérusalem. The Southeastern Universities Research Association operates the Thomas Jefferson National Accelerator Facility for the United States Department of Energy under Contract No. DE-AC05-06OR23177.

[1] D. Mueller, D. Robaschik, B. Geyer, F.M. Dittes and J. Horejsi, Fortschr. Phys. **42**, 101 (1994).
[2] X.D. Ji, Phys. Rev. Lett. **78**, 610 (1997).
[3] X.D. Ji, Phys. Rev. D **55**, 7114 (1997).
[4] A.V. Radyushkin, Phys. Lett. B **380**, 417 (1996).
[5] A.V. Radyushkin, Phys. Rev. D **56**, 5524 (1997).
[6] M. Burkardt, Phys. Rev. D **62**, 071503 (2000); **66**, 119903(E) (2002).
[7] M. Diehl, Eur. Phys. J. C **25**, 223 (2002); **31**, 277(E) (2003).
[8] A. V. Belitsky and D. Mueller, Nucl. Phys. A **711**, 118 (2002).
[9] M. Burkardt, Phys. Rev. D **72**, 094020 (2005).
[10] S. Stepanyan *et al.* (CLAS Collaboration), Phys. Rev. Lett. **87**, 182002 (2001).
[11] A. Airapetian *et al.* (HERMES Collaboration), Phys. Rev. Lett. **87**, 182001 (2001); Phys. Rev. D **75**, 011103 (2007); J. High Energy Phys. 06 (2008), 066; 11 (2009) 083; 06 (2010) 019; Phys. Lett. B **704**, 15 (2011); J. High Energy Phys. 07 (2012) 032; 10 (2012) 042.

[12] A. Airapetian *et al.* (HERMES Collaboration), Phys. Rev. C **81**, 035202 (2010).
[13] C. Adloff *et al.* (H1 Collaboration), Phys. Lett. B **517**, 47 (2001)
[14] S. Chekanov *et al.* (ZEUS Collaboration), Phys. Lett. B **573**, 46 (2003).
[15] A. Aktas *et al.* (H1 Collaboration), Eur. Phys. J. C **44**, 1 (2005).
[16] S. Chen *et al.* (CLAS Collaboration), Phys. Rev. Lett. **97**, 072002 (2006).
[17] C. Muñoz Camacho *et al.* (Jefferson Lab Hall A Collaboration), Phys. Rev. Lett. **97**, 262002 (2006).
[18] F.X. Girod *et al.* (CLAS Collaboration), Phys. Rev. Lett. **100**, 162002 (2008).
[19] M. Mazouz *et al.* (Jefferson Lab Hall A Collaboration), Phys. Rev. Lett. **99**, 242501 (2007).
[20] G. Gavalian *et al.* (CLAS Collaboration), Phys. Rev. C **80**, 035206 (2009).
[21] E. Seder *et al.* (CLAS Collaboration), Phys. Rev. Lett. **114**, 032001 (2015).
[22] M. Defurne *et al.* (Jefferson Lab Hall A Collaboration), Phys. Rev. C **92**, 055202 (2015).
[23] S. Pisano *et al.* (CLAS Collaboration), Phys. Rev. D **91**, 052014 (2015).
[24] H. S. Jo *et al.* (CLAS Collaboration), Phys. Rev. Lett. **115**, 212003 (2015).
[25] P. Joerg (COMPASS Collaboration), Proc. Sci. DIS2016, 235 (2016).
[26] K. Goeke, M.V. Polyakov and M. Vanderhaeghen, Prog. Part. Nucl. Phys. **47**, 401 (2001).
[27] M. Diehl, Phys. Rep. **388**, 41 (2003).
[28] X.D. Ji, Annu. Rev. Nucl. Part. Sci. **54**, 413 (2004).
[29] A.V. Belitsky and A.V. Radyushkin, Phys. Rep. **418**, 1 (2005).
[30] S. Boffi and B. Pasquini, Riv. Nuovo Cimento Soc. Ital. Fis. **30**, 387 (2007).
[31] M. Guidal, H. Moutarde, and M. Vanderhaeghen, Rep. Prog. Phys. **76**, 066202 (2013).
[32] E. R. Berger, F. Cano, M. Diehl, and B. Pire, Phys. Rev. Lett. **87**, 142302 (2001).
[33] F. Cano and B. Pire, Eur. Phys. J. A **19**, 423 (2004).
[34] V. Guzey and M. Siddikov, J. Phys. G **32**, 251 (2006).
[35] R. Dupré and S. Scopetta, Eur. Phys. J. A **52**, 159 (2016).
[36] O. Hen, G. A. Miller, E. Piasetzky, and L. B. Weinstein, arXiv:1611.09748 [Rev. Mod. Phys. (to be published)].
[37] P. R. Norton, Rep. Prog. Phys. **66**, 1253 (2003).
[38] D. F. Geesaman, K. Saito and A. W. Thomas, Annu. Rev. Nucl. Part. Sci. **45**, 337 (1995).
[39] J.C. Collins and A. Freund, Phys. Rev. D **59**, 074009 (1999).
[40] X.-D. Ji and J. Osborne, Phys. Rev. D **58**, 094018 (1998).
[41] V. Guzey and M. Strikman, Phys. Rev. C **68**, 015204 (2003).
[42] J. Seely *et al.*, Phys. Rev. Lett. **103**, 202301 (2009).
[43] B. A. Mecking *et al.* (CLAS Collaboration), Nucl. Instrum. Methods Phys. Res. Sect. A **503**, 513 (2003).
[44] R. Dupré *et al.*, arXiv:1706.10160.
[45] K. Hafidi *et al.*, proposal PR-08-024 to JLab PAC33 (unpublished).
[46] Y. Perrin, Ph.D. thesis, Université de Grenoble, France, 2012 [Institution Report No. 2012GRENY092].
[47] M. Hattawy, Ph.D. thesis, Université Paris Sud - Paris XI, France, 2015 [Institution Report No. 2015PA112161].
[48] A. V. Belitsky, D. Mueller, and A. Kirchner, Nucl. Phys. B **629**, 323 (2002).
[49] A. Kirchner and D. Mueller, Eur. Phys. J. C **32**, 347 (2003).
[50] A. V. Belitsky and D. Mueller, Phys. Rev. D **79**, 014017 (2009).
[51] W. Armstrong *et al.*, arXiv:1708.00888.
[52] S. Liuti and S.K. Taneja, Phys. Rev. C **72**, 032201 (2005).
[53] V. Guzey (private communication); Phys. Rev. C **78**, 025211 (2008).
[54] V. Guzey and T. Teckentrup, Phys. Rev. D **74**, 054027 (2006).
[55] M. Vanderhaeghen, P.A.M. Guichon, and M. Guidal, Phys. Rev. Lett.**80** 5064 (1998); Phys. Rev. D **60**, 094017 (1999); K. Goeke, M.V. Polyakov, and M. Vanderhaeghen, Prog.Part. Nucl. Phys. **47**, 401 (2001); M. Guidal, M.V. Polyakov, A.V. Radyushkin, and M. Vanderhaeghen, Phys. Rev. D **72**, 054013 (2005).
[56] I. V. Musatov and A. V. Radyushkin, Phys. Rev. D **61**, 074027 (2000).
[57] J. O. Gonzalez-Hernandez, S. Liuti, G. R. Goldstein, and K. Kathuria, Phys. Rev. C **88**, 065206 (2013).